

## STUDY OF CRYSTALLIZATION PROCESS IN V-SUBSTITUTED FINEMET ALLOYS

Vladimír KOLESÁR\*, Vladimír GIRMAN\*, Pavol SOVÁK\*, Karel SAKSL\*\*

\*Institute of Physics, P.J. Safarik University, Park Angelinum 9, 041 54 Košice, Slovak Republic, e-mail: vladimir.kolesar@upjs.sk

\*\*Institute of Material Research, Slovak Academy of Science, Watsonova 47, 041 00 Košice, Slovak Republic

### ABSTRACT

Nanocrystalline soft magnetic alloys can be produced by partial crystallization of amorphous precursor. The aim of this paper was to study the influence of Nb substitution by vanadium (V) in  $Fe_{73.5}Cu_1Nb_{3-x}V_xB_9Si_{13.5}$  ( $x=1.5, 3$ ) alloys on their crystallization process and the glass forming ability because the growth of the  $\alpha$ -Fe(Si) crystals is reduced by (Nb) diffusion barrier. Amorphous ribbons were prepared by melt-spinning technique. Crystallization process of amorphous alloys was examined by Different thermal analysis (DTA) in order to determine the crystallization temperatures and by X-ray powder diffraction measurements (XRD). Atomic pair correlation function  $G(r)$  and Radial distribution function  $R(r)$  has been calculated for better characterisation of as-quenched samples. It was found that higher V content accelerates crystallization process and causes worse glass forming ability. From DTA measurement was found decreasing of crystallization temperatures with higher V content.

**Keywords:** soft magnetic materials, glass forming ability, nanocrystalline structure, Atomic pair correlation function, Radial distribution function, X-ray powder diffraction

### 1. INTRODUCTION

Nanocrystalline material prepared from amorphous state, well known as FINEMET ( $Fe_{73.5}Cu_1Nb_3B_9Si_{13.5}$ ) has excellent magnetic properties, for example high permeability ( $\mu \sim 10^5$ ) and low value of coercivity ( $H_c \leq 1 A.m^{-1}$ ) [1, 2, 3, 4, 5, 6]. The possible application of this alloy includes magnetic parts of power transfers, solenoid valves, magnetic sensors, magnetic shields, actuators and so on [7]. This alloy is produced by control annealing of amorphous precursor (one hour at the temperature 550 °C). Cu atoms acts as nucleation centres of the  $\alpha$ -Fe(Si) phase during annealing process (above 500 °C). Slowly diffusing Nb atoms in amorphous phase inhibits the grain growth of  $\alpha$ -Fe(Si) phase, because of their large atomic diameter (1.429 Å) in comparison to other atoms attended in this alloy [8, 9, 10]. For that reason, the size of  $\alpha$ -Fe(Si) grains is a few nanometres. In this way, the alloy in optimal nanocrystalline state consist of nanoscale  $\alpha$ -Fe(Si) grains, amorphous phase and Nb diffusion barrier. A number of scientists have investigated the effect of Nb substitution by other elements on the magnetic properties of this alloy, but no significant improvements of this alloy were reported [6, 11, 12]. Lu et al. found that the microstructure and soft magnetic properties of  $Fe_{73.5}Cu_1Nb_{3-x}V_xSi_{13.5}B_9$  nanocrystalline alloys are strongly effect by the addition of V element [13]. The best soft magnetic properties (permeability 135 000, coercivity 0.79 A.m<sup>-1</sup>, saturation field 1.26 T) have been obtained at 1.5 at. % of V content [13]. The aim of this work was to study the influence of substitution of Nb atoms by V atoms on the crystallization process of  $Fe_{73.5}Cu_1Nb_{3-x}V_xSi_{13.5}B_9$  ( $x=1.5, 3$ ) alloys.

### 2. SUBJECT

For better characterisation of as-quenched samples, the pair function  $G(r)$  [14] and radial distribution function  $R(r)$  has been calculated. With using Fourier transformation from reciprocal (Q) space to real (r) space, the  $G(r)$  function has been calculated as:

$$G(r) = \int_{Q_{min}}^{Q_{max}} Q [S(Q) - 1] \cdot \sin(Qr) dQ \quad (1)$$

where:  $S(Q)$  - total structure factor.  $S(Q)$  can be obtained from the elastically scattered intensity  $I_e(Q)$  as:

$$S(Q) = \frac{I_e(Q) - \langle f^2(Q) \rangle}{\langle f(Q) \rangle^2}, \quad (2)$$

$$\langle f(Q) \rangle^2 = \left( \sum_i c_i f_i(Q) \right)^2,$$

$$\langle f^2(Q) \rangle = \sum_i c_i f_i^2(Q),$$

$$Q = \frac{4\pi \cdot \sin \theta}{\lambda},$$

where:  $Q$  – momentum transfer,  $\theta$  – angle of scattered radiation,  $\lambda$  – wavelength of used radiation,  $c_i$  – concentration of atoms of type  $i$ .

From the  $G(r)$  function the  $R(r)$  function has been calculated as:

$$R(r) = r \cdot G(r) + 4 \cdot \pi \cdot r^2 \cdot \rho_0, \quad (3)$$

$$\rho_0 = \frac{N_A}{\sum_i \frac{c_i M_m(i)}{\theta_i}}$$

where:  $\rho_0$  – average atomic density,  $N_A$  – Avogadro constant,  $c_i$  – concentration of atoms of type  $i$ ,  $M_m(i)$  – molar mass of the atoms,  $\theta(i)$  – density [kg.m<sup>-3</sup>]. The  $R(r)$  function provides information about the probability of finding an atom in a spherical shell at a distance  $r$  from an arbitrary atom. The average number of atoms in first

coordination shell (N) has been determined from  $R(r)$  function as:

$$N = \int_{r_1}^{r_2} R(r) dr \quad (4)$$

where:  $r_1$ ,  $r_2$  – internal and external radius of the first coordination shell [15].

The average grain size of crystalline samples is calculated from the XRD pattern using the Scherrer formula [16] as:

$$D = \frac{K \cdot \lambda}{\beta \cdot \cos \theta} \quad (5)$$

where:  $K$  – shape factor,  $\lambda$  – x-ray wavelength,  $\beta$  – line broadening at half the maximum intensity in radians,  $\theta$  – Bragg angle. The dimensionless shape factor has a typical value of about 0.9, but varies with the actual shape of the crystallite.

### 3. EXPERIMENTAL METHODS AND RESULTS

The samples in form of ribbons with chemical composition  $\text{Fe}_{73.5}\text{Cu}_1\text{Nb}_{3-x}\text{V}_x\text{Si}_{13.5}\text{B}_9$  ( $x=1.5, 3$ ) were prepared by melt-spinning technique. The structural evolution of the alloys was followed by X-ray diffraction (XRD). In-situ high temperature XRD measurements were performed in HASYLAB at DESY using Petra electron storage ring operating at the electron energy 11.28 GeV. The XRD patterns of as-quenched ribbons were collected in the temperature range from room temperature up to 800 °C with a heating rate 20 °C.min<sup>-1</sup>. The gradually annealed sample was illuminated for 30 seconds for each pattern by X-rays of wavelength  $\lambda=0.115$  Å. Two dimensional XRD patterns were recorded by 2D image plate detector. Precise radiation energy was determined by fitting a standard reference of  $\text{LaB}_6$  sample. The images taken from different stages of annealing were investigated into 2 Theta space by using Fit2D program. Differential thermal analysis (DTA) of as-quenched ribbons was performed using a SETARAM TG-DTA 92 instrument. Samples were heated up to 800 °C with a heating rate of 10 °C.min<sup>-1</sup>.

#### 3.1. Differential Thermal Analysis (DTA)

Curves presented in Fig. 1 show two exothermic peaks. The first peak represents the process of primary crystallization (formation of  $\alpha\text{-Fe}(\text{Si})$  phase) and the second peak represents the process of secondary crystallization (formation of boride phase). The temperature of primary crystallization ( $T_{x1}$ ) decreases from 485 °C to 460 °C with higher V content. The temperature of secondary crystallization ( $T_{x2}$ ) decreases from 622 °C to 578 °C with higher V content. The glass temperature ( $T_g$ ) also decreases from 315 °C to 308 °C with higher V content (see Fig. 1).

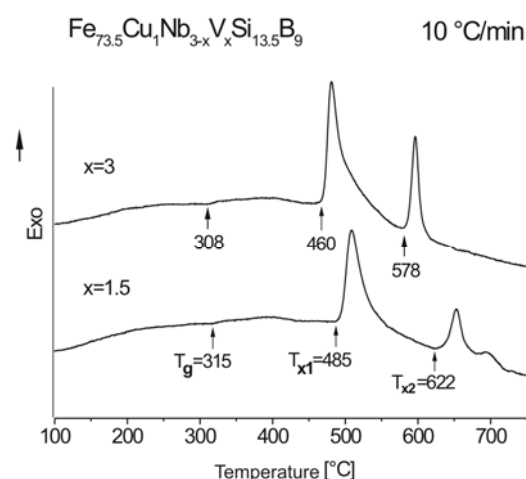


Fig. 1 DTA curves of  $\text{Fe}_{73.5}\text{Cu}_1\text{Nb}_{3-x}\text{V}_x\text{Si}_{13.5}\text{B}_9$  ( $x=1.5, 3$ ) as-quenched ribbons

#### 3.2. XRD structural analysis of as-quenched samples

The XRD distributions of  $\text{Fe}_{73.5}\text{Cu}_1\text{Nb}_{3-x}\text{V}_x\text{Si}_{13.5}\text{B}_9$  ( $x=1.5, 3$ ) as-quenched ribbons are presented in Fig. 2.

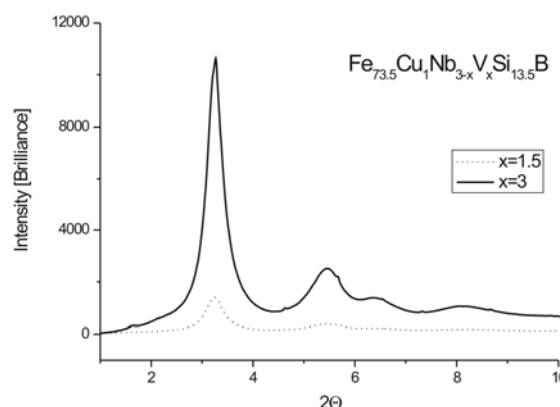
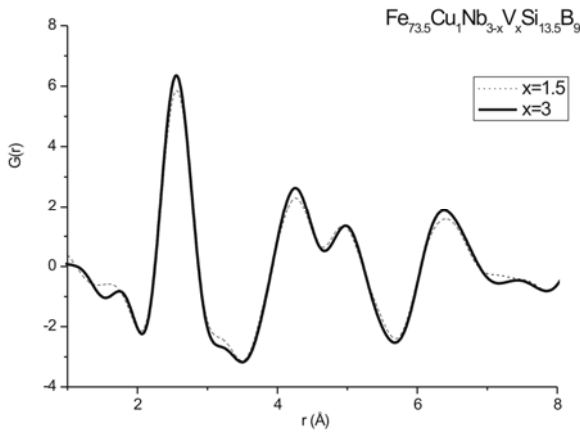


Fig. 2 XRD patterns of  $\text{Fe}_{73.5}\text{Cu}_1\text{Nb}_{3-x}\text{V}_x\text{Si}_{13.5}\text{B}_9$  ( $x=1.5, 3$ ) as-quenched ribbons

Two broad peaks can be seen in both XRD patterns what is characteristic for amorphous alloys, although in XRD pattern for  $x=3$  small discontinuities (formation of crystallites) are observable. That means that for  $x=3$  of as-quenched sample is very low content of crystalline phase. The  $G(r)$  function, given by (1), is calculated in Fig. 3. The  $G(r)$  function for  $x=1.5$  exhibits lower amplitude of peaks than for  $x=3$ , which is an indication of higher ordering with increasing V content. In the range 2-3.48 Å (first coordination shell), the main maximum of  $G(r)$  function is situated.

From the position of main maximum of  $G(r)$  function, the average distance between iron atoms has been derived. The estimated value of the Fe-Fe atoms distance is 2.56 Å for both as-quenched samples. This distance is greater than the Fe-Fe atoms distance in crystalline state (2.49 Å) due to disordering of the structure of as-quenched samples.



**Fig. 3** The G(r) function of  $Fe_{73.5}Cu_1Nb_{3-x}V_xSi_{13.5}B_9$  ( $x=1.5, 3$ ) as-quenched ribbons

The R(r) function given by (3) for  $x=1.5$  is displayed in Fig. 4.

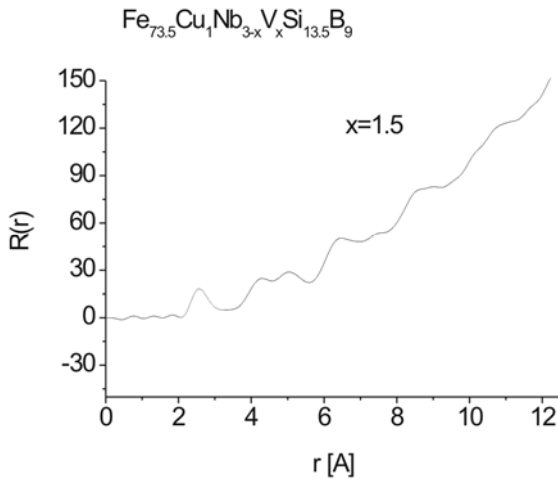


**Fig. 4** The R(r) function of  $Fe_{73.5}Cu_1Nb_{1.5}V_{1.5}Si_{13.5}B_9$  as-quenched ribbon

The area of the first peak (2-3.48 Å) is equal to average number of atoms in first coordination shell around arbitrary atom (see Fig. 4). In the first coordination shell is approximately 12 atoms for both as-quenched samples (based on the (4)), which is typical number for amorphous alloys.

**3.3. XRD structural analysis of annealed samples**

XRD patterns of  $Fe_{73.5}Cu_1Nb_{3-x}V_xSi_{13.5}B_9$  ( $x=1.5, 3$ ) samples heated on the temperature  $\sim 370$  °C are showed in Fig. 5. XRD distribution for  $x=1.5$  is still as for amorphous alloys, but the reflections from (110), (200), (211) crystallographic planes of the cubic Fe phase (PDF#6-696,  $a=2.8664$  Å, S.G.: Im3m) appears in the XRD distribution for  $x=3$  (see Fig. 5, Fig. 6 a)).

On the other hand, the DTA curves (Fig. 1) of both samples are continuous without exothermic peaks at this temperature. One of the reason of these different results can be explained by very low volume fraction of the cubic Fe phase for  $x=3$ . The chemical inhomogeneity of  $x=3$  could be the second possible reason.

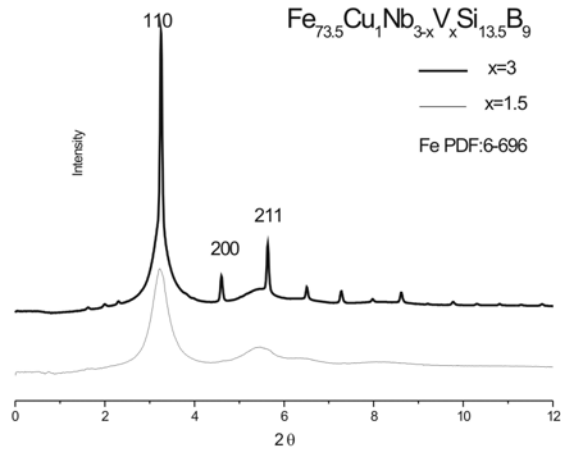


**Fig. 5** XRD patterns of  $Fe_{73.5}Cu_1Nb_{3-x}V_xSi_{13.5}B_9$  ( $x=1.5, 3$ ) samples heated on the temperature  $\sim 370$  °C

At the temperature  $\sim 470$  °C the reflections of  $Fe_3Si$  phase (PDF#42-1329,  $a=5.662$  Å, S.G.:Fm3m) and  $V_3Si$  phase (PDF#73-598,  $a=4.712$  Å, S.G.:Pm3n) were detected for  $x=3$  (see Fig. 6 b), 6 c)).

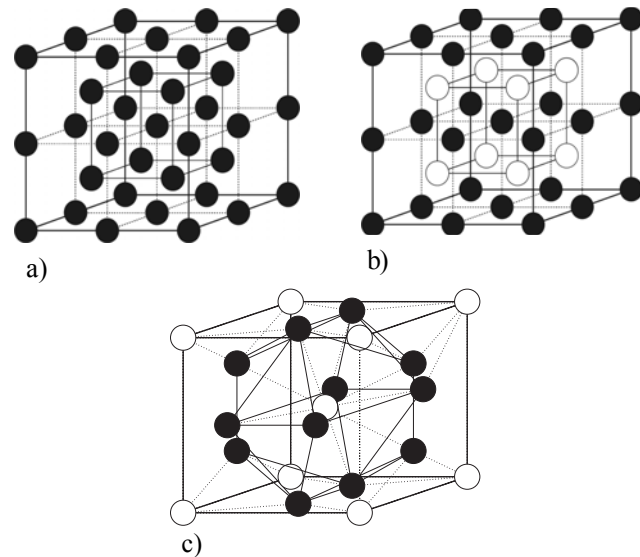


**Fig. 6** a) cubic Fe structure, b)  $Fe_3Si$  structure, black spheres signifies Fe atoms, whereas the white spheres signifies the Si atoms, c)  $V_3Si$  structure, black spheres signifies V atoms, white spheres signifies Si atoms

Crystallization process of  $Fe_2B$  phase (PDF#36-1332,  $a=4.712$  Å,  $c=4.2494$  Å, S.G.:I4/mcm) is realised in large temperature range above 520 °C.

Using the Scherrer formula (5) and eliminating the instrumental broadening of the XRD reflections, an average grain size of  $\alpha$ -Fe(Si) crystals as a function of temperature, has been estimated (see Fig. 7).

From this dependence it can be seen that the average grain size of  $\alpha$ -Fe(Si) crystals for  $x=1.5$  grows faster in shorter temperature range than the average grain size of  $\alpha$ -Fe(Si) crystals for  $x=3$ . The average grain size of  $\alpha$ -Fe(Si) crystals for  $x=3$  is stable ( $\sim 20$  nm) in whole used temperature range except for the temperature range 450 - 500 °C where (primary crystallization process (see Fig. 1)), the average grain size of  $\alpha$ -Fe(Si) crystals reaches

the values  $\sim 28$  nm. Interesting fact is that the average grain size of  $\alpha$ -Fe(Si) crystals decreases over annealing above  $\sim 460$  °C.

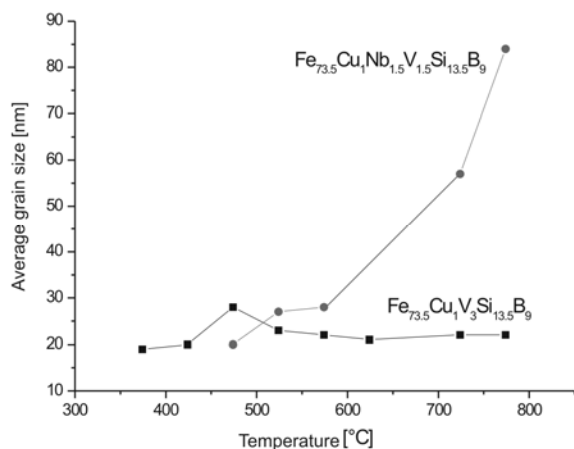


**Fig. 7** Average grain size of  $\alpha$ -Fe(Si) crystals as a function of temperature for  $\text{Fe}_{73.5}\text{Cu}_1\text{Nb}_{3-x}\text{V}_x\text{Si}_{13.5}\text{B}_9$  ( $x=1.5, 3$ ) ribbons

The coercivity dependence on the annealing temperature, with one hour of annealing time, of both experimental samples is displayed in Fig. 8.

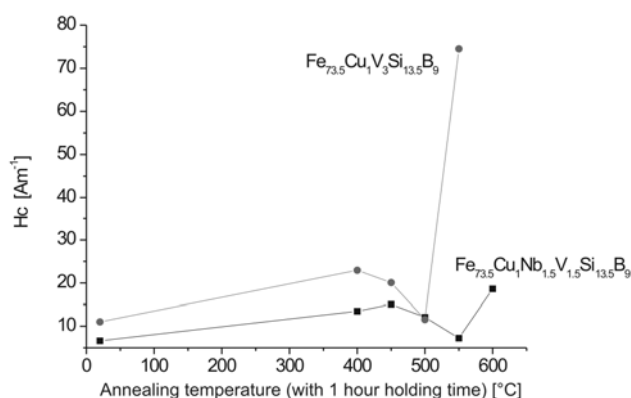


**Fig. 8** The coercivity dependence on the annealing temperature of the  $\text{Fe}_{73.5}\text{Cu}_1\text{Nb}_{3-x}\text{V}_x\text{Si}_{13.5}\text{B}_9$  ( $x=1.5, 3$ ) ribbons

From these dependences it can be seen that the best value of coercivity has been reached for the sample with  $x=3$  annealed at the temperature  $550$  °C, what is also in agreement with the results of Lu group [13].

#### 4. CONCLUSIONS

From the DTA measurement was found that the temperatures  $T_{x1}$  and  $T_{x2}$  decreases with higher V content. From the  $G(r)$  function (1) was found that in the sample with higher V content is higher degree of ordering than in  $x=1.5$  sample. In the first coordination shell ( $2-3.48$  Å) of both as-quenched samples is  $\sim 12$  atoms (equations 3, 4), which is typical number for amorphous alloys. The sample for  $x=3$  heated at the temperature  $\sim 370$  °C contains low volume fraction of the cubic Fe phase and after annealing at the temperature  $\sim 470$  °C starts crystallization of  $\text{Fe}_3\text{Si}$  phase and  $\text{V}_3\text{Si}$  phase. On the other hand the average grain size of  $\alpha$ -Fe(Si) crystals for  $x=1.5$  grows faster (from 20-

up to 80 nm) in shorter temperature range ( $450-750$  °C) than the average grain size of  $\alpha$ -Fe(Si) crystals for  $x=3$  ( $\sim 20$  nm in whole used temperature range). The average grain size of  $\alpha$ -Fe(Si) crystals decreases after reaching the annealing temperature  $\sim 460$  °C. The lowest value of coercivity has been reached for the  $x=3$  sample annealed at the temperature  $550$  °C.

From the results presented in this paper could be summarised that V content accelerates crystallization process and causes worse glass forming ability of experimental samples. V atom ( $1.321$  Å) is worse inhibitor of grain growth than Nb atom ( $1.429$  Å) is.

#### ACKNOWLEDGMENTS

This work was done in the frame of the project „Centre of Excellence of progressive materials with nano- and submicron microstructure“, with support of the Operational programme Research and Development financed from European Regional Development Fund and in the frame of internal scientific grant system of P.J. Safarik University.

#### REFERENCES

- [1] YOSHIKAWA, Y. – OGUMA, S. – YAMAUCHI, K.: New Fe-based soft magnetic alloys composed of ultrafine grain structure, *J. Appl. Phys.*, vol. 64, no. 10, pp. 6044, Nov. 1988.
- [2] HERZER, G.: Grain structure and magnetism of nanocrystalline ferromagnets, *IEEE Trans. Magn.*, vol. 25, no. 5, pp. 3327-3329, 1989.
- [3] YOSHIKAWA, Y. – YAMAUCHI, K.: Fe-based soft magnetic alloys composed of ultrafine grain structure, *Mater. Trans. Jpn. Int. Metals*, vol. 31, no. 4, pp. 307-314, Apr. 1990.
- [4] HERZER, G. – WARLIMONT, H.: Nanocrystalline soft magnetic materials by partial crystallization of amorphous alloys, *Nanostruct. Mater.*, no. 3, pp. 263-268, May 1992.
- [5] HERZER, G.: Nanocrystalline soft magnetic materials, *Phys. Scr.*, pp. 307-314, 1993.
- [6] KOLLAR, P. – FUZER, J. – MATTA, P. – SVEC, T. – KONC, M.: Magnetic properties of  $\text{Fe}_{73.5}\text{Cu}_1\text{Nb}_{3-x}\text{U}_x\text{Si}_{13.5}\text{B}_9$  ( $x=1, 2, 3$ ) nanocrystalline alloys, *J. Magn. Magn. Mater.*, pp. 213-214, 1996.
- [7] LIU, H. – WU, Y. – ZHANG, G. – YIN, CH. – DU, Y.: Variation of permeability of Nb-poor Finemet under different field amplitudes, *J. Magn. Magn. Mater.*, vol. 320, no. 10, pp. 1705-1711, May 2008.
- [8] BRZOZOVSKI, R. – WASIAK, M. – PIEKARSKI, H. – SOVAK, P. – UZNANSKI, P. – MONETA, M. E.: Properties of Mn-doped FINEMET, *J. Alloys. Compd.*, vol. 470, no. 2, pp. 5-11, Feb. 2009.
- [9] RAJA, M. M. – CHATTOPADHYAY, K. – MAJUMDAR, B. – NARAYANASAMY, A.: Structure and soft magnetic properties of Finemet alloys, *J. Alloys. Compd.*, vol. 297, no. 2, pp. 199-205, Feb. 2000.

- [10] PASZTI, Z. – SZABO, I. – KISDI-KOSZO, E. – PETO, G. – HORVATH, H. – ZSOLDOS, E. – GUCZI, L.: Preparation and characterisation of finemet amorphous magnetic thin films with enhanced Cu content, *Thin Solid Films*, vol. 317, no. 2, pp. 294-297, Apr. 1998.
- [11] PANDA, A. K. – CHATTORAJ, I. – MITRA, A.: Structural and soft magnetic properties of  $Fe_{73.5}Nb_3M_1Si_{13.5}B_9$  (M=Cu, Mn, Pt), *J. Magn. Magn. Mater.*, vol. 222, no. 3, pp. 236-270, Dec. 2000.
- [12] MCHENRY, M. E. – WILLARD, M. A. – LAUGHLIN, D. E.: Amorphous and nanocrystalline materials for applications as soft magnets, *Prog. Mater.Sci.*, vol. 44, no 4, pp. 291-433, Oct. 1999.
- [13] LU, W. – YAN, B. – LI, Y. – TANG, R.: Structure and soft magnetic properties of V-doped Finemet-type alloys, *J. Alloys. Compd.*, vol. 454, no. 2, pp. L10-L13, Apr. 2008.
- [14] FABER, T. E. – ZIMMAN, J. M.: *Philos. Mag.*, vol. 11, pp. 235, 1996.
- [15] MICHALIK, S.: *Diploma work*, pp. 21-22, March 2007.
- [16] PECHARSKY, V. K. – ZAVALIJ, P. Y.: *Fundamentals of Powder Diffraction and Structural Characterization of Materials*, pp. 171-184, 2005.

between structure and magnetic properties of the nanocrystalline alloys on the base Fe and Co at the Institute of Physics at P. J. Safarik University. His scientific research is focusing on structural evolution of amorphous and nanocrystalline alloys by X-ray diffraction with using synchrotron radiation source.

**Vladimír Girman** was born in 17.08.1980. He completed engineering study on Technical University in Kosice – Faculty of Metallurgy, in 2004. PhD diploma he gained in 2008 on the same Faculty of Metallurgy on Department of Materials Science. Dissertation thesis was oriented on research of CuZnAl shape memory alloys. Since 2008 he is employed on University of P. J. Safarik, Institute of Physics, Department of Solid State Physics as a scientist worker. He is interested in field of materials physics and electron microscopy.

**Pavol Sovák** was born in 23.09.1959. In 1983 he completed university study on University of P. J. Safarik in Kosice. In 1992 he gained PhD diploma on the same University. In 1994 he absolved post-doc position on Technical University in Eindhoven. Since 2007 he awarded professor title. Actual held positions are dean of Faculty of Science on University of P. J. Safarik (from 2003) and senior scientist. He is interested in electron microscopy, X-ray diffractometry and magnetism of solid state with emphasis on FINEMET type alloys. Besides this, he is member of International Steering Committee of XFEL project.

Received January 28, 2010, accepted July 6, 2010

## BIOGRAPHIES

**Vladimír Kolesár** was born on 16.04.1980. In 2004 he gained master of engineering diploma at the Faculty of Mining, Ecology, Process Control and Geotechnology at Technical University in Kosice. In 2007 he gained Master of Science diploma in Solid state physics at Faculty of Science of P. J. Safarik University in Kosice. In 2007 he started his PhD with the topic Study of correlation

**Karel SaksI** was born in 27.05.1974. In 1997 he awarded engineering title (Ing.) on Technical University of Kosice, Faculty of Metallurgy. He closed up PhD study in 2000 in Slovak Academy of Science, Institute of Materials Research. During 2001 and 2002 – 2007 he took post-doc positions in Department of Physics, Technical University of Denmark and HASYLAB at DESY, respectively. In the present he is employed in Slovak Academy of Science - Institute of Materials as a senior researcher. Main goal of his work is synthesis, characterization of nanostructured materials and their adaptation to engineering praxis.